View metadata, citation and similar papers at core.ac.uk
brought to you by CORE
provided by CONICET Digital

Accepted Article

Article

TRPV4 contributes to resting membrane potential in Retinal Müller cells: Implications in cell volume regulation†

Vanina Netti#, Juan Fernández#, Maia Kalstein, Alejandro Pizzoni, Gisela Di Giusto, Valeria Rivarola, Paula Ford and Claudia Capurro*

# These authors contributed equally to this work.

Laboratorio de Biomembranas, IFIBIO Houssay, CONICET-UBA, Departamento de Ciencia Fisiológicas, Facultad de Medicina, Universidad de Buenos Aires, Argentina.

***Corresponding author:** Prof. Claudia Capurro, Ph.D. Laboratorio Biomembranas, *IFIBIO Houssay, CONICET-UBA*, Departamento de Ciencias Fisiológicas. Facultad de Medicina, Universidad de Buenos Aires. Paraguay 2155, piso 7 (1121) Buenos Aires, ARGENTINA. TEL: 54-11-59509500 (ext. 2145). e-mail: *capurro@retina.ar*

Running Head: TRPV4 and Müller cell volume regulation

Key Words: TRPV4; Human Müller Cells; Membrane Potential; Intracellular Calcium Levels; Cell Volume Regulation.

Grant information: This work was supported by grants from Universidad de Buenos Aires, Argentina; Grant number UBACYT 20020100100648 and Consejo Nacional de Ciencia y Tecnología (CONICET), Argentina; Grant Number: PIP 0296

†This article has been accepted for publication and undergone full peer review but has not been through the copyediting, typesetting, pagination and proofreading process, which may lead to differences between this version and the Version of Record. Please cite this article as doi: [10.1002/jcb.25884]

Additional Supporting Information may be found in the online version of this article.

Received 28 October 2016; Revised 12 January 2017; Accepted 13 January 2017
Journal of Cellular Biochemistry
This article is protected by copyright. All rights reserved
DOI 10.1002/jcb.25884

Accepted Article

Abstract

Neural activity alters osmotic gradients favoring cell swelling in retinal Müller cells. This swelling is followed by a regulatory volume decrease (RVD), partially mediated by an efflux of KCl and water. The transient receptor potential channel 4 (TRPV4), a nonselective calcium channel, has been proposed as a candidate for mediating intracellular Ca^{2+} elevation induced by swelling. We previously demonstrated in a human Müller cell line (MIO-M1) that RVD strongly depends on ion channel activation and, consequently, on membrane potential (V_m). The aim of this study was to investigate if Ca^{2+} influx via TRPV4 contributes to RVD by modifying intracellular Ca^{2+} concentration and/or modulating V_m in MIO-M1 cells. Cell volume, intracellular Ca^{2+} levels, and V_m changes were evaluated using fluorescent probes. Results showed that MIO-M1 cells express functional TRPV4 which determines the resting V_m associated with K^+ channels. Swelling-induced increases in Ca^{2+} levels was due to both Ca^{2+} release from intracellular stores and Ca^{2+} influx by a pathway alternative to TRPV4. TRPV4 blockage affected swelling-induced biphasic response (depolarization-repolarization), suggesting its participation in modulating V_m changes during RVD. Agonist stimulation of Ca^{2+} influx via TRPV4 activated K^+ channels hyperpolarizing V_m and accelerating RVD. We propose that TRPV4 forms a signaling complex with Ca^{2+} and/or voltage-dependent K^+ channels to define resting V_m and V_m changes during RVD. TRPV4 involvement in RVD depends on the type of stimuli and/or degree of channel activation, leading to a maximum RVD response when Ca^{2+} influx overcomes a threshold and activates further signaling pathways in cell volume regulation.

This article is protected by copyright. All rights reserved

Accepted Article

Introduction

A major functional role of Müller cells is to control extracellular osmotic and ionic homeostasis in the retina (Kofuji and Newman, 2004; Bringmann et al., 2006; Reichenbach and Bringmann, 2010). During intense neural activity, retinal cells can be surrounded by a hypo-osmotic environment, since light-evoked changes in the ionic composition of the extracellular space cause a decrease in osmolarity, thus favoring glial swelling (Dmitriev et al., 1999). This swelling is followed by a regulatory volume decrease response (RVD), mediated by an iso-osmotic efflux of KCl, organic osmolytes and water through Aquaporin-4 (AQP4), a dynamic process resulting from the concerted action of volume-sensing mechanisms and intricate signaling cascades directed at initiating multiple adaptations (Hirrlinger et al., 2008; Wurm et al., 2006; Pannicke et al., 2004).

The increase of cytosolic Ca^{2+} concentration is a widespread consistent cellular response to hypo-osmotic swelling, with contributions from both extracellular Ca^{2+} influx and Ca^{2+} release from intracellular stores (Pasantes-Morales et al., 2006; Pasantes-Morales and Morales-Mulia, 2008). However, RVD is Ca^{2+}-dependent in some cell types and Ca^{2+}-independent in others. In the first cases, increases in cytosolic Ca^{2+} modulate Ca^{2+}-activated K^+ channels, mainly large-conductance Ca^{2+}-activated K^+ channels (BK), to elicit K^+ efflux. In contrast, in another large number of cell types, these channels are not involved in RVD. In these cases, K^+ efflux occurs through other types of K^+ channels, such as voltage-gated K^+ (K_v) channels or swelling-activated K^+ channels (inwardly rectifying K^+ channels Kir or two-pore–domain K^+ channels) (Stutzin and Hoffmann, 2006; Pasantes-Morales 2016). Other RVD mechanisms, such as the volume-sensitive anion channel and osmolyte efflux pathways, are also often Ca^{2+}-independent (Pasantes-Morales et al., 2006). Though glial cells exhibit a rise in intracellular Ca^{2+} concentration in response to hypo-osmotic stimuli, the RVD and osmolyte fluxes involved in this process are not always Ca^{2+}-dependent (Benfenati et al., 2011; Pasantes-Morales et al., 2006; Morales-Mulia et al., 1998; O'Connor and Kimelberg, 1993). It is therefore not surprising that the channels involved in RVD may be different, even in the same cell type, and cells may respond to a single or several signals elicited by volume change, such as depolarization, membrane stretch and/or elevation of intracellular Ca^{2+}.

This article is protected by copyright. All rights reserved

In astrocyte glial cells, the Transient Receptor Potential Vanilloid type 4 (TRPV4), a calcium-permeable nonselective cation channel, was proposed as a mediator in the swelling-induced elevation of intracellular Ca^{2+} related to cell volume regulation (Butenko et al., 2012; Benfenati et al., 2011). Nevertheless, a recent study suggests that TRPV4 and Ca^{2+} do not seem to be essential for RVD to occur (Mola et al., 2015). Until recently, the participation of TRPV4 in the RVD of Müller glial cells was less explored. It is now reported that TRPV4 channels traduce mouse Müller cell volume increases into physiological responses (Ryskamp et al., 2014). Jo et al. (2015) proposed that water influx through the water channel AQP4 drives Ca^{2+} influx via TRPV4 in the glial end foot of mouse Müller cells. This regulates the expression of AQP4 and Kir4.1 K^+ channels and facilitates the time course and amplitude of hypotonicity-induced swelling and RVD. However, the authors concluded that TRPV4 might contribute only to adaptive volume regulation in retinal glia (Jo et al., 2015). We have recently shown in a human retinal Müller cell line (MIO-M1) that the efficiency of the RVD process depends not only on the activation of ion channels, but is also strongly modulated by concurrent changes in resting membrane potential (V_m) (Fernández et al., 2013). Although Müller cells express different types of K^+ channels, it is well accepted that near resting V_m, Kir4.1 and BK, are the major channels involved in K^+ homeostasis (Puro et al., 1996; Reichenbach and Bringmann, 2010). Since TRPV4 functionally couples to Ca^{2+}-sensitive K^+ channels in many tissues (White et al., 2016; Jo et al., 2015; Ma et al., 2013; Sullivan and Earley, 2013; Early et al., 2005), it is likely that Ca^{2+} influx via TRPV4 may contribute to RVD response by altering intracellular Ca^{2+} concentration and/or by modulating V_m. Therefore, the aim of this study was to further investigate the participation of TRPV4 in the RVD response using a human Müller cell line. We propose that in MIO-M1 cells TRPV4 forms a signaling complex with $Ca^{2+}$and/or voltage-dependent K^+ channels to define not only resting V_m but also changes in V_m that occur during RVD. The contribution of TRPV4 to RVD depends on the type of stimuli and/or degree of channel activation, with a maximum RVD response when Ca^{2+} influx overcomes a threshold and activates additional signaling pathways for cell volume regulation.

This article is protected by copyright. All rights reserved

Accepted Article

Accepted Article

Materials and Methods

Cell Cultures

The MIO-M1 cell line (kindly provided by Dr. Astrid Limb, University College London, London, UK) is a spontaneously immortalized retinal Müller glial cell line, originated from human retina, that retains many characteristics of Müller cells (Limb et al., 2002). Cells were grown as monolayers in the presence of Dulbecco's Modified Eagle Medium (DMEM) / glutamax supplemented with 10% fetal bovine serum (FBS), containing 5 µg/ml streptomycin and 5 U/ml penicillin at 37°C in a humidified atmosphere containing 5% CO_2. Cells were routinely subcultured every week, and those to be studied were grown on coverslips during 3-4 days before recording.

For immunofluorescence and functional studies, MIO-M1 cells were seeded on glass coverslips (diameter 1.2 cm) at 5-10 x 10^3 cells/ml densities for 48 hours and then subjected to different experimental conditions.

Measurement of Cell Volume Changes, RVD and Intracellular Ca^{2+}

By using the Ca^{2+}-sensitive dye Fura-2 AM and recording at the Ca^{2+}-sensitive (380 nm) and -insensitive (358 nm, isosbestic) wavelengths, we simultaneously recorded changes in cell volume and $[Ca^{2+}]_i$ in single cells. MIO-M1 cells grown on coverslips were mounted on a chamber, incubated in 14 µM Fura 2-AM (Molecular Probes Inc) for 60 minutes at 37ºC and then washed to remove excess dye. To prevent dye compartmentalization upon loading, Pluronic F127 (0.2%) (Molecular Probes Inc) was used to dissolve the Fura 2-AM dye. The coverslips were again incubated in the experimental buffer for 15 minutes before the experiments. The chamber was placed on the stage of a Nikon TE-200 epifluorescence inverted microscope (Nikon Planfluor 40X oil immersion objective lens) as previously described (Ford et al., 2005). Fluorescence was collected from a small circular region (pinhole) of 1-3% of the total area of the cell, localized in the central region of the cell. F was inversely proportional to the external osmolarity and showed a linear correlation with the relative external osmolarity. The coverslips were incubated in the experimental buffer at 20ºC for at least 15 min before the experiment. Fluorescence data were acquired every 10 seconds at 20ºC using a charge coupled device camera (Hamamatsu C4742-

This article is protected by copyright. All rights reserved

95) connected to a computer with the Metafluor data acquisition software (Universal Imaging Corporation, PA). During experiments, bathing solution was exchanged by aspirating the media and adding new media.

As previously reported, changes in cell volume were read from the fluorescence intensity recorded at the isosbestic wavelength of 358 nm and changes in $[Ca^{2+}]_i$ were obtained from the ratio of 358/380 (R_t/R_0 Fura-2) (Altamirano et al., 1998; Mualem et al., 1992). For calibration, cells were sequentially exposed to solutions with different osmolalities and relative fluorescence (F_t/F_0) was recorded. F_0 represents the signal obtained from each pinhole when placed in equilibrium with an iso-osmotic medium with an osmolality OsM_0 (300 mOsM). F_t is the fluorescence from the same region at time *t*, when placed in equilibrium with a solution with an osmolality of OsM_t (range: 200 to 400 mOsM). A linear relationship between F_0/F_t and the relative external osmolality (OsM_0/OsM_t) was obtained (Supplementary Figure 1). Changes in cell volume were calculated as follows:

$$\frac{V}{V_0} = \frac{\left(\frac{F_0}{F_t}\right) - f_b}{1 - f_b}$$

where V is cell volume at time t; V_0 is cell volume at t = 0 and F_0/F_t is relative fluorescence. The relative background (f_b) is the y intercept of a plot of F_0/F_t versus OsM_0/OsM_t and represents the relative fluorescence distributed in the intracellular compartments, which is not sensitive to osmotic changes.

RVD after cell exposure to a hypo-osmotic medium was calculated by the following equation:

$$RVD_t = \left[\frac{\left(\frac{V}{V_0}\right)_{max} - \left(\frac{V}{V_0}\right)_t}{\left(\frac{V}{V_0}\right)_{max} - 1} \right] \times 100$$

where $(V/V_0)_{max}$ is the maximal value of V/V_0 attained during hypo-osmotic swelling (peak), and $(V/V_0)_t$ represents the value of V/V_0 observed at time t. RVD_t thus denotes the magnitude of volume regulation at time t, with 100% RVD indicating complete volume regulation and 0 % RVD indicating no volume regulation.

Measurement of Membrane Voltage Changes

This article is protected by copyright. All rights reserved

Accepted Article

Transmembrane potential was measured using bis-(1,3-dibutylbarbituric acid) trimethine oxonol ($DIBAC_4(3)$, Molecular Probes), a slow response anionic dye, whose emission has been shown to be independent of cell volume changes, as previously used for MIO-M1 cells (Fernández et al., 2013). The intracellular concentration of $DIBAC_4(3)$ depends on V_m following a Nernstian distribution (Brauner et al., 1984; Epps et al., 1994). Cells were loaded with 2.5 μM $DIBAC_4(3)$ for 15 minutes at 20ºC and placed on the stage of the same microscope described in the previous section. Excitation wavelength was 490 nm. Emitted light (above 520 nm) was recorded at 10 second intervals. Fluorescence intensity was monitored until it reached stable values before starting the experiments. Fluorescence intensity changes after interventions were relativized to stationary values (F_0/F_t) and data were corrected for background noise and drift.

MIO-M1 resting V_m is -63.1 ± 2.3 mV as previously reported (Fernández et al., 2013). 1% changes in fluorescence correspond to a V_m variation of 2.2 mV, as calculated from the mean calibration curve (0.0045 ± 0.002, X ± SD, n= 58).

Western blotting studies

Confluent MIO-M1 cells were washed three times in cold PBS and were incubated for 30 min at 4°C in a cold lysis buffer containing 150 mM NaCl, 20 mM Tris/HCl, pH 7.5, 5 mM EDTA, 1% Triton 100, 1 mM PMSF, 5 μg/ml aprotinin, 10 μg/ml antipain, 10 μg/ml leupeptin and 10 μg/ml pepstatin. Cells were then collected with a rubber scraper, homogenized and sonicated. Cell lysates were subjected to electrophoresis in 8% SDS-polyacrylamide gel (Bio-Rad), transferred to a nitrocellulose membrane (Bio-Rad) and blocked 1 hour with 5% non-fat dried skimmed milk in PBS-T (80 mMNa_2HPO_4, 20 mMNaH_2PO_4, 100 mM NaCl and 0.1% Tween 20, pH 7.5). Membranes were incubated with the rabbit polyclonal TRPV4 antibody (1/1000), generated against a peptide corresponding to amino acids 853–871 of rat TRPV4, (Alomone Labs, #ACC-034) overnight at 4°C. The blots were then washed and incubated 1h at room temperature with a goat anti-rabbit IgG conjugated to horseradish peroxidase (dilution 1:7500; Sigma–Aldrich St. Louis, MO, U.S.A). Membranes were visualized using the chemiluminescence method (SuperSignal Substrate, Pierce) and captured on a Gbox (Syngene, Frederick, MD).

This article is protected by copyright. All rights reserved

Accepted Article

Accepted Article

Immunofluorescence Assays

Colocalization of TRPV4 and the specific plasma membrane marker Alexa Fluor 488-conjugated wheat germ agglutinin (WGA; Molecular Probes) were performed. Cells were first stained with WGA, at 4ºC for 30 minutes to label the surface glycoproteins of the plasma membrane. Then, cells were fixed in 3% paraformaldehyde for 30 min, washed with PBS and neutralized with NH_4Cl for 30 min. Cells were permeabilized for 30 min with 0.2% Triton X-100 at room temperature and washed with PBS. Samples were blocked with 1% Bovine Serum Albumin (BSA) and incubated with anti-TRPV4 (1/1500; Alomone Labs, #ACC-034) overnight at 4ºC. Next, cells were washed and incubated with Cy3-conjugated goat anti-rabbit IgG (1/200, Jacson Immuno, 111-165-003) for 2 h at room temperature. Coverslips were mounted with Vectashield mounting medium.

Images were captured using confocal Olympus FV1000 microscope and digitized. Fluorescence intensity was quantified per cell, identified by Hoechst nuclei staining. Ten fields were analyzed per experiment and quantified by densitometric analysis using Image J-software. Since plasma membrane TRPV4 expression was low, to identify its presence, we created a mask of plasma membrane as previously described (Janecki et al., 2000). Briefly, WGA images were binarized so that the signal from WGA was ascribed the value of “1” and the rest of the image was ascribed the value of “0”. The Boolean logical operation “AND” was then performed on the corresponding images, representing signals from TRPV4-Cy3 and from WGA (binary mask). This resulted in generation of a new image (shown in yellow in the figures) in which only the TRPV4-Cy3 fluorescent signal corresponding to the membrane was present. Images were also analyzed by using colocalization tools and estimated using the M2 superposition coefficient of Manders (SCM), which measures the fraction of WGA that overlaps TRPV4 signal, and is described by the following equation

$$SCM = \frac{\Sigma_i (R_i x G_i)}{\sqrt{\Sigma_i R_i^{\,2} x G_i^{\,2}}}$$

A value of 1 indicates 100% of superposition between signals of colocalized pixels, while a value of 0 indicates absence of colocalization.

This article is protected by copyright. All rights reserved

Accepted Article

Solutions and Chemicals

For functional experiments, cells were first set for at least 10 minutes in an external iso-osmotic solution containing (mM): 126 NaCl; 5,5 KCl; 2,5 $CaCl_2$; 1,25 $MgCl_2$; 20 Hepes and 10 Glucose (Osmolarity: 299 ± 2 mOsM). Calcium-free solutions were made by adding EGTA (1 mM) and replacing $CaCl_2$ by $MgCl_2$. Experiments varying extracellular K^+ concentration were done by replacing NaCl with KCl. Hypo-osmotic solutions were prepared from iso-osmotic solution by the removal of NaCl (Osmolarity: 200 ± 2 mOsM). All solutions were titrated to pH 7.40 using NaOH (Sigma-Aldrich), and osmolalities were routinely measured by a pressure vapor osmometer (Wescor).

In some experiments, 1 mM $BaCl_2$; 1 mM Tetraethylammonium (TEA) and 0.2 μM Apamin were used to block K^+ channels. TRPV4 activation or inhibition were tested with 10 μM of TRPV4 specific activator 4α-Phorbol-12,13-didecanoate (4α-PDD) and 10 μM TRPV4 specific inhibitor RN1734, respectively. Since in the presence of the RN1734 we identified up to a 10% change in fluorescence levels, we considered this as a threshold for response to 4α-PDD. Additional experiments were performed using 3 nM of TRPV4 specific agonist GSK1016790A (GSK101) and 0,5 nM of TRPV4 specific antagonist HC-067047 (HC-06). Finally, 1 μM of endoplasmic reticulum (ER) Ca^{2+} ATPase inhibitor Thapsigargin (TG) was used to deplete intracellular Ca^{2+} stores. All drugs were purchased from Sigma-Aldrich. Cells were pre-incubated in an iso-osmotic extracellular solution containing drugs or vehicle (DMSO). 1 mM Fura-2 and 0.6 mM $DIBAC_4(3)$ stock solutions were prepared in DMSO and stored at -20°C until used.

Statistics

Values are reported as mean ± SEM, and n is the number of cells evaluated in each condition. Student's t test for unpaired data was used according to each protocol; $p < 0.05$ was considered a significant difference.

This article is protected by copyright. All rights reserved

Accepted Article

Results

MIO-M1 cells express functional TRPV4 in the plasma membrane

Using western blot and immunofluorescence assays, the first set of experiments evaluated TRPV4 expression and plasma membrane localization in MIO-M1 cells. Western blot analysis revealed a band of ~100 kDa, corresponding to TRPV4 (Figure 1A). Figure 1B shows a representative immunofluorescence experiment, with anti-TRPV4 antibodies (red) and the cell membrane marker WGA (green), revealing a large intracellular TRPV4 signal and a minor fraction of the stain that co-localizes with WGA (yellow). To test whether this small plasma membrane TRPV4 expression had functional significance, intracellular Ca^{2+} levels were monitored by videomicroscopy with Fura-2 ratio, using the TRPV4 specific activator, 4α-PDD. Addition of 10 µM 4α-PDD elicited a robust and transient increase in intracellular Ca^{2+} levels in 72 ± 5% of cells (Figure 1C). This effect was eliminated in the absence of external Ca^{2+} (Figure 1D) or in cells pretreated with 10 µM RN1734, a selective TRPV4 antagonist (Figure 1E). Similar results were obtained using a structurally different agonist GSK-1016790A (GSK101, 3 nM) or the antagonist HC-067047 (HC-06, 0.5 nM) (Figure 1F). Altogether, molecular and functional results confirmed the expression of active TRPV4 channels in MIO-M1 cells.

TRPV4 contributes to resting membrane potential in MIO-M1 cells

Our previous studies in Müller cells, showed that RVD response is strongly modulated by changes in the electrochemical gradient for K^+ and Cl^- and, thus, by V_m (Fernandez et al., 2013). Keeping in mind that the high K^+ permeability of the plasma membrane is the basis of the very negative resting V_m of Müller cells and that TRPV4 plays a key role in modulating Ca^{2+}-activated K^+ channels in a variety of cell types, we investigated the putative contribution of TRPV4 in modulating the resting V_m in MIO-M1 cells. Cells were loaded with $DIBAC_4(3)$ and V_m was monitored by videomicroscopy before and after the addition of 10 µM RN1734 or different blockers of K^+ channels: i- 1 mM $BaCl_2$; ii- 1 mM TEA (a concentration shown to be selective for BK channels in Müller cells) or iii- 0.2 µM Apamin, a blocker of SK channels (Reichenbach & Bringmann, 2010). Figure 2A shows the time course of F_t/F_0 $DIBAC_4(3)$ of MIO-M1 cells under iso-

This article is protected by copyright. All rights reserved

osmotic conditions, where TRPV4 inhibition elicited a robust plasma membrane depolarization. As expected, Figure 2B illustrates that incubation of cells with increasing concentrations of external K^+ induced V_m depolarization in a concentration-dependent manner, but the slope of this response was significantly decreased in the presence of RN1734, suggesting that TRPV4 modulates K^+ permeability. As depicted in Figure 2C, plasma membrane depolarization was observed not only with RN1734 but also by blocking Ba^{2+}-sensitive K^+ channels or BK Ca^{2+}-activated K^+ channels with TEA. In contrast, inhibition of SK Ca^{2+}-activated K^+ channels with apamin did not modify $\Delta F_t/F_0$, dismissing the contribution of these channels to resting V_m. Altogether these data strongly suggest that TRPV4 may contribute to resting V_m in Müller cells by a functional interaction with Ca^{2+} and/or V_m-sensitive K^+ channels.

TRPV4 modulates V_m changes occurring during RVD

We next investigated the contribution of TRPV4 to changes in cytosolic Ca^{2+} concentration, $\%RVD_{10}$ and V_m after hypo-osmotic swelling in MIO-M1 cells. First we evaluated if the plasma membrane localization of TRPV4 was altered after cell exposure to a hypo-osmotic media (ΔOsM ± 100 mOsM), as described in other systems (Galizia et al., 2012). Figure 3A shows that there were no changes in TRPV4 signal after 10 minutes of hypo-osmotic shock (Fluorescence intensity per cell, red channel, ISO: 889.3 ± 80.4 vs HYPO 822.0 ± 55.6, 15-20 cells of 7-11 fields, n=3 experiments, NS) or in the fraction of TRPV4 that co-localizes with the plasma membrane marker WGA (yellow) in these experimental conditions (Mander´s coefficient, Plasma Membrane TRPV4 vs. WGA: ISO 0.283 ± 0.019 vs. HYPO 0.325 ± 0.024, 15-20 cells of 7-11 fields, n=3 experiments, NS). Figure 3B shows the time course of relative changes in Ca^{2+} levels (R_t/R_0 Fura-2) when cells were exposed to the hypo-osmotic media. It can be observed that cell swelling led to an increase in Ca^{2+} levels that was not affected by the presence of 10 µM RN1734 (Figure 3B insert), suggesting that TRPV4 does not contribute to this change in Ca^{2+} levels. In addition, Figures 3C illustrates that neither the kinetics of relative cell volume changes (V/V_0) nor cell volume regulation (insert, $\%RVD_{10}$) were affected by TRPV4 blockage. However, in Figure 4A we show that the swelling-induced biphasic response (depolarization-repolarization) was partially absent in the presence of RN1734, suggesting the contribution of TRPV4 to these changes. Moreover, while swelling-

This article is protected by copyright. All rights reserved

Accepted Article

induced depolarization was not affected by K^+ channels blockers, the magnitude of the repolarization was significantly reduced by Ba^{2+} and TEA to similar levels as with RN1734, but not by Apamin (Figure 4B).

All these results strongly suggest that even if TRPV4 is not involved in the hypo-osmotic-induced Ca^{2+} increase, it contributes to modulate changes in V_m that occur during RVD almost certainly associated with major K^+ channels expressed in Müller cells, Kir4.1 and BK.

Intracellular Ca^{2+} stores play a fundamental role in RVD response

Since an increase in cytosolic Ca^{2+} concentration may be attributed to both extracellular Ca^{2+} influx and Ca^{2+} release from intracellular stores, we further investigated the origin of cell swelling-induced Ca^{2+} increase in MIO-M1 cells. Figure 6A shows that the kinetics of intracellular Ca^{2+} increase during the hypo-osmotic shock (ΔOsM ± 100 mOsM) was notably modified in the absence of external Ca^{2+}. In fact, in a Ca^{2+}-free solution, the swelling-induced Ca^{2+} increase was transient and significantly reduced in comparison to control conditions (Figure 5A, insert), suggesting that intracellular Ca^{2+} changes induced by hypotonicity depend, at least partially, on extracellular Ca^{2+}. However, Figure 5B shows that external Ca^{2+} removal did not affect the kinetics of V/V_0 nor cell volume regulation response ($\%RVD_{10}$), as compared to control conditions. Afterwards, we evaluated whether intracellular Ca^{2+} stores participate in cell volume regulation. With that aim, we treated cells with thapsigargin (TG), a non-competitive inhibitor of the endoplasmic reticulum (ER) Ca^{2+}-ATPase (SERCA), which causes the depletion of intracellular Ca^{2+} stores. Figure 5C shows that in a Ca^{2+}-free solution, TG induced a transient increase in Fura-2 R_t/R_0 and then Ca^{2+} levels returned to basal values, as cells are unable to induce a Ca^{2+} entry to refill ER stores. In contrast, in the presence of external Ca^{2+}, TG treatment induces a putative store-operated Ca^{2+} Entry (SOCE) evidenced by a sustained increase in intracellular Ca^{2+} levels. The cells subsequent exposure to a hypo-osmotic shock (ΔOsM ± 100 mOsM), in the presence of TG but in the absence of extracellular Ca^{2+}, caused a significant decreased in intracellular Ca^{2+} levels (Figure 5C insert). However, in the presence of extracellular Ca^{2+}, TG maintained intracellular Ca^{2+} levels always higher than basal levels (Figure 6C insert). Interestingly, Figure 5D shows that the kinetics of V/V_0 was also quite different with TG treatment in the presence or absence of external Ca^{2+}. TG

This article is protected by copyright. All rights reserved

Accepted Article

significantly enhanced RVD as compared to control conditions in a Ca^{2+} containing solution, but this response was almost completely impaired in the absence of external Ca^{2+} (Figure 5D insert). Altogether, these results propose that swelling-induced increase in Ca^{2+} levels are due to both Ca^{2+} entry from extracellular media and Ca^{2+} release from ER stores. However, only endogenous Ca^{2+} stores play a key role in MIO-M1 cell volume regulation.

Agonist-induced activation of TRPV4 enhance RVD response

Since the osmotic swelling-induced increase in Ca^{2+} levels in MIO-M1 cells was small (~4-5 %), we tested if activation of TRPV4 by an alternative pathway may contribute to modulate RVD. Therefore, to measure intracellular Ca^{2+} levels and RVD we stimulated TRPV4 with 10 µM of 4α-PDD prior to the hypo-osmotic shock. Figures 6A shows that the increase in intracellular Ca^{2+} levels after TRPV4 activation was not significantly augmented by the exposure of cells to a hypo-osmotic shock, but this huge rise in intracellular Ca^{2+} produced a rapid cell volume recovery with the consequent increase in $\%RVD_{10}$ (Figure 6B and insert). These changes in Ca^{2+} and RVD responses were completely reverted in the absence of external Ca^{2+} (Figure 6C and D). In addition, Figure 7A illustrates that 4α-PDD induced a hyperpolarization in iso-osmotic conditions. The changes in V_m evoked by the osmotic swelling (depolarization-repolarization) did not occur in the presence of 4α-PDD which provoked a higher hyperpolarization. TRPV4-agonist induced hyperpolarization was prevented in the presence of K^+-channels blockers Ba^{2+} and TEA (Figure 7B).

Altogether, these results indicate that selective activation of TRPV4 during hypo-osmotic shock with the agonist 4α-PDD causes a larger Ca^{2+} influx, activating K^+ channels, then, hyperpolarizing cells, accelerating the RVD response.

Discussion

The present work provides new insights regarding the contribution of TRPV4 channels to RVD response in retinal human Müller cells (MIO-M1 cells). We observed the expression of a small fraction of TRPV4 at the plasma membrane, but also a large intracellular TRPV4 signal.

This article is protected by copyright. All rights reserved

Accepted Article

However, the activation of TRPV4 induced huge increases in Ca^{2+} levels, demonstrating that functional TRPV4 channels are present in the plasma membrane of MIO-M1 cells. Interestingly, five splice variants have been described for human TRPV4 (bands migrating at 86-100 kDa), some of which lack Ankyrin domains and are retained intracellularly (Arniges et al., 2006). However, we detected a single isoform of TRPV4 at ~100 kDa in MIO-M1 cell line. Whether intracellular localization is because TRPV4 appears in these compartments as intermediates of biosynthetic pathways or if they are active participants in signal transduction and/or membrane trafficking, as previously reported (Dong et al., 2010; White et al., 2016), must be further investigated.

We demonstrate that TRPV4 contributes to define the resting V_m of Müller cells since specific blockage of the channel induced plasma membrane depolarization, indicating that TRPV4 is a tonically-active channel. Given that inhibition of TRPV4-mediated Ca^{2+} currents should lead *per se* to membrane hyperpolarization, and not to the observed depolarization, we hypothesize that in Müller cells TRPV4 works in concert with K^+ channels, just as it does in other systems (Ma et al., 2013; Sullivan and Earley, 2013; Early et al, 2005). Even if Müller cells express different types of K^+ channels, such as voltage-gated K^+ channels and Ca^{2+}-activated K^+ channels, it is well accepted that at the resting V_m, K^+ permeability is mediated by Ba^{2+}-sensitive inwardly rectifying K^+ channels (Kir4.1), which are key players in retinal K^+ homeostasis along with BK channels (Puro et al., 1996). Kir4.1 and BK channels are well discernible due to their different electrophysiological properties (Reichenbach and Bringmann, 2010). In Müller cells, BK channels are mainly activated by an increase in the free Ca^{2+} level at the intracellular side of the plasma membrane as well as by membrane depolarization. We provide evidence that blockade of K^+ channels with Ba^{2+} evoked a depolarization similar to that induced by TRPV4 inhibition, and TEA also induced a depolarization, but to a lesser extent than Ba^{2+}. Therefore, it is likely that TRPV4, in concert with activation of one or more K^+ channels, contributes to define resting V_m in MIO-M1 cells. We propose that Ca^{2+} influx via TRPV4 may activate Ca^{2+}-dependent BK channels but at the same time Ca^{2+} influx induces a transient depolarization that, in turn, may increase Kir4.1 outwardly directed K^+ currents at V_m more positive than resting V_m in Müller cells (Reichenbach and Bringmann, 2010).

Our data also demonstrates that, as in many other cell types, MIO-M1 cells had increased intracellular Ca^{2+} levels during osmotic swelling. However, this increase was slight (~5%) and

This article is protected by copyright. All rights reserved

Accepted Article

occurred through a pathway other than TRPV4. External Ca^{2+} removal significantly reduced swelling-activated increases in Ca^{2+} levels without affecting RVD, suggesting the contribution of RVD effectors independently of extracellular Ca^{2+} influx, at least in these experimental conditions. These data differ from studies on rodent Müller glia, which conclude that TRPV4 is the main mediator of hypotonic-induced Ca^{2+} entry (Ryskamp et al., 2014; Jo et al., 2015), but agree with the final suggestion that TRPV4 is not necessarily involved in RVD. The reasons for these discrepant results are unclear but might be due to differences between species, cell models, experimental means of detection of intracellular Ca^{2+} and/or size of the hypotonic stimuli. However, our results are consistent with previous data from mouse-cultured astrocytes in which the inhibition of TRPV4 or the removal of extracellular Ca^{2+} did not affect RVD (Mola et al., 2016; Morales-Mulia et al., 1998). Mola et al. (2016) concluded that the rapid AQP4-dependent cell swelling is the main determinant of RVD efficiency. Nevertheless, there are also reports in astrocytes showing that AQP4 is functionally coupled to TRPV4 (Benfenati et al., 2011). We did not focus our present work on evaluating the role of AQP4 association with TRPV4 during a hypotonic shock in MIO-M1 cells since our previous results showed that the removal of AQP4 from the plasma membrane affects osmotic water permeability and RVD without altering TRPV4 expression or function (unpublished results). In line with this observation, we here showed that TRPV4 activation or inhibition did not modify cell swelling kinetics, probably indicating the absence of a functional interaction between TRPV4 and AQP4 to determine RVD, as previously reported in mouse Müller cells (Jo et al., 2015). However, we cannot disregard that this interaction may occur to define other pathophysiological processes. In fact, previous reports in mouse Müller cells described that TRPV4 absence or overactivation as well as AQP4 deletion are associated with reactive gliosis and gliovascular modifications (Ryskamp et al., 2014, Nicchia et al., 2016) which are, in turn, associated with alterations in Ca^{2+} homeostasis.

We also suggest that a possible alternative pathway for Ca^{2+} increase during a hypo-osmotic challenge in MIO-M1 cells could be Ca^{2+} release from stores, as previously shown in astrocytes (Morales-Mulia et al., 1998; Mola et al., 2015). In fact, our data demonstrated that RVD largely depended on intracellular Ca^{2+} stores, probably indicating that intracellular Ca^{2+} release may be sufficient to elicit the RVD response and could explain the insensitivity of RVD to external Ca^{2+} in

This article is protected by copyright. All rights reserved

Accepted Article

MIO-M1 cells. A recent work showed that store-operated signalling represents a major source of cytosolic Ca^{2+} in mouse Müller cells; however, the physiological relevance of this finding has not yet been established (Molnar et al., 2016). The likely purpose of extracellular Ca^{2+} entry during a hypo-osmotic challenge may be the replenishment of endogenous stores, which are depleted after swelling.

The lack of contribution of TRPV4 to the increase of Ca^{2+} levels under a hypo-osmotic stimulation in MIO-M1 cells does not rule out the possibility that TRPV4 may participate in RVD response when it is largely activated by agonists, as shown by other authors (Cardin et al, 2003).

We demonstrated that stimulation of Ca^{2+} influx via TRPV4 enhanced RVD to a greater extent than observed in control conditions. A similar response was observed when intracellular Ca^{2+} stores were depleted in the presence of extracellular Ca^{2+}, activating SOCE. Finally, we found a positive correlation between changes in intracellular Ca^{2+} levels and % RVD (r^2: 0.7012; n = 100 cells). Therefore, we propose that RVD machinery involves both Ca^{2+}-independent and Ca^{2+}-dependent machinery in MIO-M1 cells. When Ca^{2+} levels enhance over those induced by a physiological hypo-osmotic swelling, a more potent RVD takes place due to the opening of other Ca^{2+}-activated channels. In line with this idea, there are reports in astrocytes that indicate that increasing intracellular [Ca^{2+}] over hypo-osmotic-induced levels by the ionophore ionomycin or by activation of G-protein coupled receptors markedly potentiates some of the osmolyte efflux pathways (Cardin et al. 2003; Vazquez Juarez et al., 2008).

Interestingly, our observation of a functional association between TRPV4 and Ca^{2+} and/or V_m-sensitive K^+ channels to define resting V_m in MIO-M1 cells, opens the question about its contribution to the depolarization-repolarization that takes place during an osmotic shock. Our results show that cell swelling-induced depolarization was significantly reduced with TRPV4 antagonist. Since this depolarization is due to concurrent events, such as intracellular ions dilution, Ca^{2+} influx and/or Cl^- efflux (Fernandez et al., 2013), it would be expected to be affected by reductions in the K^+ driving force by dilution and blocking Ca^{2+} influx via TRPV4. RVD-induced repolarization was inhibited to the same extent by blocking TRPV4 or blocking K^+ channels with Ba^{2+} or TEA, suggesting a functional association of TRPV4 and BK channels during RVD. This relationship was further confirmed when TRPV4 was activated by the agonist 4α-PDD during a

This article is protected by copyright. All rights reserved

Accepted Article

hypo-osmotic shock, which causes cell hyperpolarization, that was completely blunted by Ba^{2+} or TEA.

How could TRPV4 blockage affect V_m without evoking detectable changes in the magnitude of cytosolic Ca^{2+} levels or in the %RVD during the osmotic shock? We have previously demonstrated that in MIO-M1 cells, as in many other systems, only a fraction of RVD is mediated by KCl efflux: there is also a major component (~70%) mediated by organic osmolyte efflux (Fernández et al., 2013; Ando et al., 2012; Pasantes-Morales et al., 1994). Therefore it is likely that hypo-osmotic-induced local changes in Ca^{2+} conductance mediated by TRPV4 occur close to the plasma membrane and do not affect intracellular Ca^{2+} levels, though they are sufficient for BK channel activation. In fact, it has been reported that in local Ca^{2+} microdomains, Ca^{2+} concentration can rapidly rise to very high levels, often up to orders of magnitude greater than bulk cytoplasmatic Ca^{2+}, providing means for rapid and selective activation of targets closeby, such as Ca^{2+}-activated K^+ channels (Parekh, 2008). Parallely, other Ca^{2+}-dependent and independent mechanisms could be activated to evoke RVD response. Previous studies in human Müller cells have shown that RVD also depends on ATP activation of purinergic receptors P2Y, which elicits an increase in intracellular Ca^{2+} levels (Reichenbach & Bringmann 2016). Moreover, it was reported that TRPV4 activation evokes ATP release in several systems (White et al., 2016). Hence, there may be a link between TRPV4 and purinergic receptor activation during RVD. Future experiments are necessary to address this issue.

In summary, our data reveal that TRPV4 in association with K^+ channels not only defines steady-state V_m but also modulates changes in V_m occurring during a hypo-osmotic shock. This functional association is mediated by Ca^{2+} influx via TRPV4. We also propose that the involvement of TRPV4 in RVD response depends on the type of stimuli and/or degree of channel activation, leading to a maximum RVD response when Ca^{2+} influx overcomes a threshold to activate further signalling pathways for cell volume regulation. Altogether, these findings add new insights into knowledge on the role of TRPV4 in the retinal Müller cells.

This article is protected by copyright. All rights reserved

Accepted Article

Accepted Article

Acknowledgments

The authors thank Dr. Astrid Limb (University College London, London, UK) for providing the human Müller Cell Line (MIO-M1), María Teresa Politi and Jessica Haefner for language assistance.

References

1. Altamirano J, Brodwick MS, Alvarez-Leefmans FJ. 1998. Regulatory volume decrease and intracellular Ca2+ in murine neuroblastoma cells studied with fluorescent probes. J Gen Physiol 112:145-60.
2. Ando D, Kubo Y, Akanuma S, Yoneyama D, Tachikawa M, Hosoya K. 2012. Function and regulation of taurine transport in Müller cells under osmotic stress. Neurochem Int 60:597-604.
3. Arniges M, Fernández-Fernández JM, Albrecht N, Schaefer M, Valverde MA. 2006. Human TRPV4 channel splice variants revealed a key role of ankyrin domains in multimerization and trafficking. J Biol Chem 281:1580-6.
4. Benfenati V, Caprini M, Dovizio M, Mylonakou MN, Ferroni S, Ottersen OP, Amiry-Moghaddam M. 2011. An aquaporin-4/transient receptor potential vanilloid 4 (AQP4/TRPV4) complex is essential for cell-volume control in astrocytes. Proc Natl Acad Sci 8;108:2563-8.
5. Bräuner T, Hülser DF, Strasser RJ. 1984. Comparative measurements of membrane potentials with microelectrodes and voltage-sensitive dyes. Biochim Biophys Acta 11;771:208-16.
6. Bringmann A, Pannicke T, Grosche J, Francke M, Wiedemann P, Skatchkov SN, Osborne NN, Reichenbach A. 2006. Müller cells in the healthy and diseased retina. Prog Retin Eye Res 25:397-424.
7. Butenko O, Dzamba D, Benesova J, Honsa P, Benfenati V, Rusnakova V, Ferroni S, Anderova M. 2012. The increased activity of TRPV4 channel in the astrocytes of the adult rat hippocampus after cerebral hypoxia/ischemia. PLoS One 7:e39959.

This article is protected by copyright. All rights reserved

Accepted Article

8. Cardin V, Lezama R, Torres-Márquez ME, Pasantes-Morales H. 2003. Potentiation of the osmosensitive taurine release and cell volume regulation by cytosolic Ca2+ rise in cultured cerebellar astrocytes. Glia 44:119-28.

9. Dmitriev AV, Govardovskii VI, Schwahn HN, Steinberg RH. 1999. Light induced changes of extracellular ions and volume in the isolated chick retina-pigment epithelium preparation. Vis Neurosci 16:1157-1167.

10. Dong XP, Wang X & Xu H. 2010. TRP Channels of Intracellular Membranes. J Neurochem 113:313-328.

11. Earley S, Heppner TJ, Nelson MT, Brayden JE. 2005. TRPV4 forms a novel Ca2+ signaling complex with ryanodine receptors and BKCa channels. Circ Res 9;97:1270-9.

12. Epps DE, Wolfe ML, Groppi V. 1994. Characterization of the steady-state and dynamic fluorescence properties of the potential-sensitive dye bis-(1,3-dibutylbarbituric acid) trimethine oxonol (Dibac4(3)) in model systems and cells. Chem Phys Lipids 69:137-50.

13. Fernández JM, Di Giusto G, Kalstein M, Melamud L, Rivarola V, Ford P, Capurro C. 2013. Cell volume regulation in cultured human retinal Müller cells is associated with changes in transmembrane potential. PLoS One 8(2):e57268.

14. Ford P, Rivarola V, Chara O, Blot-Chabaud M, Cluzeaud F, Farman N, Parisi M, Capurro C. 2005. Volume regulation in cortical collecting duct cells: role of AQP2. Biol Cell 97:687-97.

15. Galizia L, Pizzoni A, Fernandez J, Rivarola V, Capurro C, Ford P. 2012. Functional interaction between AQP2 and TRPV4 in renal cells. J Cell Biochem 113:580-9.

16. Hirrlinger PG, Wurm A, Hirrlinger J, Bringmann A, Reichenbach A. 2008. Osmotic swelling characteristics of glial cells in the murine hippocampus, cerebellum, and retina in situ. J Neurochem 105:1405-17. doi: 10.1111/j.1471-4159.2008.05243

17. Janecki AJ1, Janecki M, Akhter S, Donowitz M. 2000. Quantitation of plasma membrane expression of a fusion protein of Na/H exchanger NHE3 and green fluorescence protein (GFP) in living PS120 fibroblasts. J Histochem Cytochem 48:1479-92.

18. Jo AO, Ryskamp DA, Phuong TT, Verkman AS, Yarishkin O, MacAulay N, Križaj D. 2015. TRPV4 and AQP4 Channels Synergistically Regulate Cell Volume and Calcium Homeostasis in Retinal Müller Glia. J Neurosci 30;35:13525-37.

This article is protected by copyright. All rights reserved

19. Kofuji P, Newman EA. 2004. Potassium buffering in the central nervous system. Neuroscience 129:1045-56.
20. Limb GA, Salt TE, Munro PM, Moss SE, Khaw PT. 2002. In vitro characterization of a spontaneously immortalized human Müller cell line (MIO-M1). Invest Ophthalmol Vis Sci 43(3):864-9.
21. Ma X, Du J, Zhang P, Deng J, Liu J, Lam FF, Li RA, Huang Y, Jin J, Yao X. 2013. Functional role of TRPV4-KCa2.3 signaling in vascular endothelial cells in normal and streptozotocin-induced diabetic rats. Hypertension 62:134-139.
22. Mola MG, Sparaneo A, Gargano CD, Spray DC, Svelto M, Frigeri A, Scemes E, Nicchia GP. 2016. The speed of swelling kinetics modulates cell volume regulation and calcium signaling in astrocytes: A different point of view on the role of aquaporins. Glia 64:139-54.
23. Molnár T, Yarishkin O, Luso A, Barabas P, Jones B, Marc RE, Phuong TT, Križaj D. 2016. Store-Operated Calcium Entry in Müller Glia Is Controlled by Synergistic Activation of TRPC and Orai Channels. J Neurosci 36:3184-98.
24. Morales-Mulia S, Vaca L, Hernandez-Cruz A, Pasantes-Morales H. Osmotic swelling-induced changes in cytosolic calcium do not affect regulatory volume decrease in rat cultured suspended cerebellar astrocytes. 1998. J Neurochem 71:2330-8.
25. Muallem S, Zhang BX, Loessberg PA, Star RA. 1992. Simultaneous recording of cell volume changes and intracellular pH or Ca2+ concentration in single osteosarcoma cells UMR-106-01. J Biol Chem 267:17658-17664.
26. Nicchia GP, Pisani F, Simone L, Cibelli A, Mola MG, Dal Monte M, Frigeri A, Bagnoli P, Svelto M. 2016. Glio-vascular modifications caused by Aquaporin-4 deletion in the mouse retina. Exp Eye Res 146:259-68.
27. O'Connor ER, Kimelberg HK. 1993. Role of calcium in astrocyte volume regulation and in the release of ions and amino acids. J Neurosci 13:2638-50.
28. Pannicke T, Iandiev I, Uckermann O, Biedermann B, Kutzera F, Wiedemann P, Wolburg H, Reichenbach A, Bringmann A. 2004. A potassium channel-linked mechanism of glial cell swelling in the postischemic retina. Mol Cell Neurosci 26:493-502.

This article is protected by copyright. All rights reserved

Accepted Article

29. Parekh AB. 2008. Ca2+ microdomains near plasma membrane Ca2+ channels: impact on cell function. J Physiol 586:3043–3054.

30. Pasantes-Morales H. Channels and Volume Changes in the Life and Death of the Cell 2016. Mol Pharmacol 90:358–370.

31. Pasantes-Morales H, Chacón E, Murray RA, Morán J. Properties of osmolyte fluxes activated during regulatory volume decrease in cultured cerebellar granule neurons. J Neurosci Res. 1994 15;37(6):720-7.

32. Pasantes-Morales H, Lezama RA, Ramos-Mandujano G, Tuz KL. 2006. Mechanisms of cell volume regulation in hypo-osmolality. Am J Med 119:S4-11.

33. Pasantes-Morales H, Morales Mulia S. Influence of calcium on regulatory volume decrease: role of potassium channels. 2008 Nephron 86:414-27.

34. Puro DG, Yuan JP, Sucher NJ. 1996. Activation of NMDA receptor-channels in human retinal Müller glial cells inhibits inward-rectifying potassium currents. Vis Neurosci 13:319-326.

35. Reichenbach A, Bringmann A. 2010. Müller Cells in the Healthy and Diseased Retina. New York:Springer. P.35-213.

36. Reichenbach A, Bringmann A. 2016. Role of Purines in Müller Glia. J Ocul Pharmacol Ther 32:518-533.

37. Ryskamp DA, Jo AO, Frye AM, Vazquez-Chona F, MacAulay N, Thoreson WB, Križaj D. 2014. Swelling and eicosanoid metabolites differentially gate TRPV4 channels in retinal neurons and glia. J Neurosci 19;34:15689-700.

38. Stutzin A, Hoffmann EK. 2006. Swelling-activated ion channels: functional regulation in cell-swelling, proliferation and apoptosis. Acta Physiol 187:27-42.

39. Sullivan MN, Earley S. 2013. TRP channel Ca(2+) sparklets: fundamental signals underlying endothelium-dependent hyperpolarization. Am J Physiol Cell Physiol 15;305:C999-C1008.

40. Vázquez-Juárez E, Ramos-Mandujano G, Hernández-Benítez R, Pasantes-Morales H. 2008. On the role of G-protein coupled receptors in cell volume regulation. Cell Physiol Biochem 21:1-14.

This article is protected by copyright. All rights reserved

Accepted Article

41. White JPM, Cibelli M, Urban L, Nilius B, McGeown JG, Nagy I. 2016. TRPV4: Molecular Conductor of a Diverse Orchestra. Physiol Rev 96:911–973.
42. Wurm A, Pannicke T, Iandiev I, Wiedemann P, Reichenbach A, Bringmann A. 2006. The developmental expression of K+ channels in retinal glial cells is associated with a decrease of osmotic cell swelling. Glia 54:411-23.

Accepted Article

This article is protected by copyright. All rights reserved

Accepted Article

Legend to figures

Figure 1: TRPV4 expression and functionality in MIO-M1 cells. A- Western blot showing TRPV4 expression. **B-** Representative confocal images of MIO-M1 cells immunostained for TRPV4 (Cy3, red) and for the cell plasma membrane marker WGA-Alexa Fluor 488 (green). Image showing TRPV4 expressed at the plasma membrane (PM TRPV4, yellow) generated by a mask of plasma membrane (see Methods). Scale bar, 10 µm. **C and D-** Representative recordings of intracellular Ca^{2+} levels with Fura-2 AM (R_t/R_0 Fura-2) in cells exposed, at the arrow, to 10 µM 4α-PDD (TRPV4 specific agonist) in the presence of 2.5 mM of external $CaCl_2$ ($+Ca^{2+}$) or in the absence of external Ca^{2+} ($0Ca^{2+}$). **E-** Representative recordings of intracellular Ca^{2+} levels with Fura-2 AM in cells pretreated with 10 µM RN1734 (TRPV4 antagonist), and then with 10 µM 4α-PDD + 10 µM RN1734 and finally removing RN1734 (Insert: enlarged y-scale to show the effects of RN1734 during the first 25 min). **F-** Maximal variation in intracellular Ca^{2+} levels (Δmax R_t/R_0 Fura-2) for cells treated with vehicle, 10 µM 4α-PDD, 3 nM GSK101, 10 µM RN1734 + 10 µM 4α-PDD or 0.5 nM HC-06 + 10 µM 4α-PDD. Three independent assays were performed for each experimental condition including 19-29 cells per experiment.

Figure 2: Contribution of TRPV4 to resting membrane potential in MIO-M1 cells. V_m was monitored using the dye $DIBAC_4(3)$ under different experimental conditions. **A-** Representative kinetics of relative fluorescence changes, F_t/F_0 $DIBAC_4(3)$, when cells were exposed, at the arrow, to 10 µM of the TRPV4 antagonist RN1734 or vehicle (DMSO). **B-** Slope x 10^{-4}, $F_t/F_0 DIBAC_4(3)$ x mM^{-1}: Vehicle 79.1 ± 2.8 vs RN1734 48.0 ± 4.1, $p<0.001$, n=9-18 cells from 4 experiments. **C-** Maximal change in fluorescence obtained after pretreatment of cells with: Vehicle, 10 µM RN1734 or different blockers of K^+ channels (1 mM $BaCl_2$; 1 mM TEA or 0.2 µM Apamin). Values are mean ± SEM from 3-4 experiments including a total of 40-91 cells; ***p < 0,001 vehicle vs. RN1734 or Ba^{2+}; ** p < 0,01 vehicle vs. TEA.

Figure 3: Role of TRPV4 on swelling-induced Ca^{2+} levels and RVD.

This article is protected by copyright. All rights reserved

MIO-M1 cells were subjected to a hypo-osmotic stress (ΔOsM = 100 mOsM) in the presence of 10 µM RN1734 or vehicle (DMSO). Intracellular Ca^{2+} levels and cell volume changes were measured in cells loaded with Fura 2-AM **A-** Representative confocal images of cells showing TRPV4 distribution before and after 10 minutes exposure to hypo-osmotic media. Cells were immunolabeled with anti-TRPV4 (red) and the cell plasma membrane marker WGA-Alexa Fluor 488 (green). Plasma membrane fraction was obtained for TRPV4-Cy3 fluorescent signal (PM TRPV4, yellow). Scale bar, 10 µm. **B-** Kinetics of changes in relative Fluorescence (R_t/R_0 Fura-2) after the hypo-osmotic shock showing that RN1734 do not affect swelling-induced Ca^{2+} levels increase. *Insert:* mean values of the percentage of intracellular Ca^{+2} levels increase for both experimental conditions. **C-** Dynamics of relative cell volume changes (V/V_0) in the presence of RN1734 or vehicle (DMSO). *Insert:* mean values of $\%RVD_{10}$ for both experimental conditions. Values are mean ± SEM for 40-46 cells of 4 independent experiments.

Figure 4: Effects of blockage of TRPV4 on swelling-induced changes in V_m. MIO-M1 cells were subjected to a hypo-osmotic stress (ΔOsM = 100 mOsM) in the presence of 10 µM RN1734 or vehicle (DMSO). **A-** Representative kinetics of changes in relative fluorescence (F_t/F_0) using $DIBAC_4(3)$, when cells were exposed to the hypo-osmotic stress in both experimental conditions. **B-** $\Delta F_t/F_0$ $DIBAC_4(3)$ mean values of maximal fluorescence changes (Depolarization) obtained after pretreatment of cells with: 10 µM RN1734 or different blockers of K^+ channels (1 mM $BaCl_2$; 1 mM TEA or 0.2 µM Apamin). The magnitude of the Repolarization was assessed as the difference between $\Delta F_t/F_0$ at the maximum peak and $\Delta F_t/F_0$ 30 minutes after exposure to a hypo-osmotic media. Values are mean ± SEM for 25-47 cells from 3-6 independent experiments *** $p < 0.001$ vehicle vs. RN1734, Ba^{2+} or TEA.

Figure 5: Contribution of extracellular and intracellular Ca^{2+} to RVD. MIO-M1 cells were loaded with Fura 2-AM to measure intracellular Ca^{2+} levels and cell volume changes. Cells were exposed to a hypo-osmotic stress (ΔOsM = 100 mOsM, HYPO) **A-** Kinetics of changes in relative fluorescence (R_t/R_0 Fura-2) in cells subjected to a hypo-osmotic stress in the presence ($+Ca^{2+}$) or

This article is protected by copyright. All rights reserved

Accepted Article

absence of external Ca^{2+} ($0Ca^{2+}$). *Insert:* mean values of the percentage of intracellular Ca^{+2} levels increase for both experimental conditions. Values are mean ± SEM for 28-67 cells from 4 independent experiments, *** $p < 0.001$ $+Ca^{2+}$ vs. $0Ca^{2+}$ **B-** Dynamics of relative cell volume changes in cells subjected to a hypo-osmotic in the presence ($+Ca^{2+}$) or absence of external Ca^{2+} ($0Ca^{2+}$). *Insert:* mean values of $\%RVD_{10}$ for both experimental conditions. Values are mean ± SEM for 28-67 cells from 4 independent experiments, *** $p < 0.001$ $+Ca^{2+}$ vs. $0Ca^{2+}$. **C-** To deplete intracellular Ca^{2+} stores, cells were first incubated with 1 µM TG in the presence ($+Ca^{2+}$) or in the absence of Ca^{2+} ($0Ca^{2+}$) followed by the hypo-osmotic shock. *Insert*: Percentage of intracellular Ca^{2+} increase 20 minutes after the addition of 1 µM TG in the absence or in the presence of external Ca^{2+} (TG + Ca^{2+} and TG $0Ca^{2+}$ respectively). Values are mean ± SEM for 42-61 cells from 3-4 independent experiments, *** $p < 0.001$ TG $+Ca^{2+}$ Vs TG $0Ca^{2+}$. **D-** Kinetics of relative cell volume Changes (V/V_0) in cells exposed to all conditions described in C. *Insert:* Mean values of $\%RVD_{10}$ in the presence or absence of external Ca^{2+} when cells were incubated with 1 µM TG (TG + Ca^{2+} and TG $0Ca^{2+}$ respectively). Values are mean ± SEM for 42-61 cells from 3-4 experiments. *** $p < 0.001$ TG $+Ca^{2+}$ vs TG $0Ca^{2+}$.

Figure 6: Effect of TRPV4 activation on swelling-induced Ca^{2+} levels and RVD. Intracellular Ca^{2+} levels and cell volume changes were measured in cells loaded with Fura 2-AM and subjected to a hypo-osmotic stress (ΔOsM = 100 mOsM) in the presence of 10 µM 4α-PDD or vehicle (DMSO). **A-C** Representative experiments showing the kinetic of intracellular Ca^{2+} levels, as relative fluorescence changes (F_t/F_0 Fura-2), in the presence **(A)** or absence of external Ca^{2+} **(C)**. **B-** Kinetic of cell volume changes, as relative fluorescence changes (F_t/F_0), in the presence or absence of 4α-PDD or vehicle. **D-** Kinetic of cell volume changes, as relative fluorescence changes (F_t/F_0), in the presence of 4α-PDD with ($+Ca^{2+}$) or without ($0Ca^{2+}$) external Ca^{2+}. *Inserts in B and D:* Mean values of % of RVD at 10 minutes after the osmotic shock ($\%RVD_{10}$) in both experimental conditions. Values are mean ± SEM for 40-91 cells from 3-5 independent experiments ** $p < 0.01$ vehicle vs. 4α-PDD and 4α-PDD + Ca^{2+} vs. 4α-PDD, $0Ca^{2+}$.

This article is protected by copyright. All rights reserved

Accepted Article

Figure 7: Effects of TRPV4 activation on swelling-induced changes in V_m. MIO-M1 cells were loaded with $DIBAC_4(3)$ and subjected to a hypo-osmotic stress (ΔOsM = 100 mOsM) in the presence of 10 µM 4α-PDD or vehicle (DMSO). **A-** Kinetics of changes in relative fluorescence (F_t/F_0) when cells were exposed to a hypo-osmotic stress in the presence of 4α-PDD or control (vehicle). **B-** Mean values of maximal fluorescence changes ($\Delta F_t/F_0$ $DIBAC_4(3)$) during the osmotic challenge in cells treated with vehicle (DMSO), 4α-PDD, 4α-PDD + Ba^{2+} or 4α-PDD + TEA. Values are mean ± SEM for 40-91 cells from 3-5 independent experiments *** $p < 0.001$ vehicle vs. 4α-PDD and ### $p < 0.001$ 4α-PDD + Ca^{2+} vs. 4α-PDD, $0Ca^{2+}$.

Accepted Article

This article is protected by copyright. All rights reserved

Accepted Article

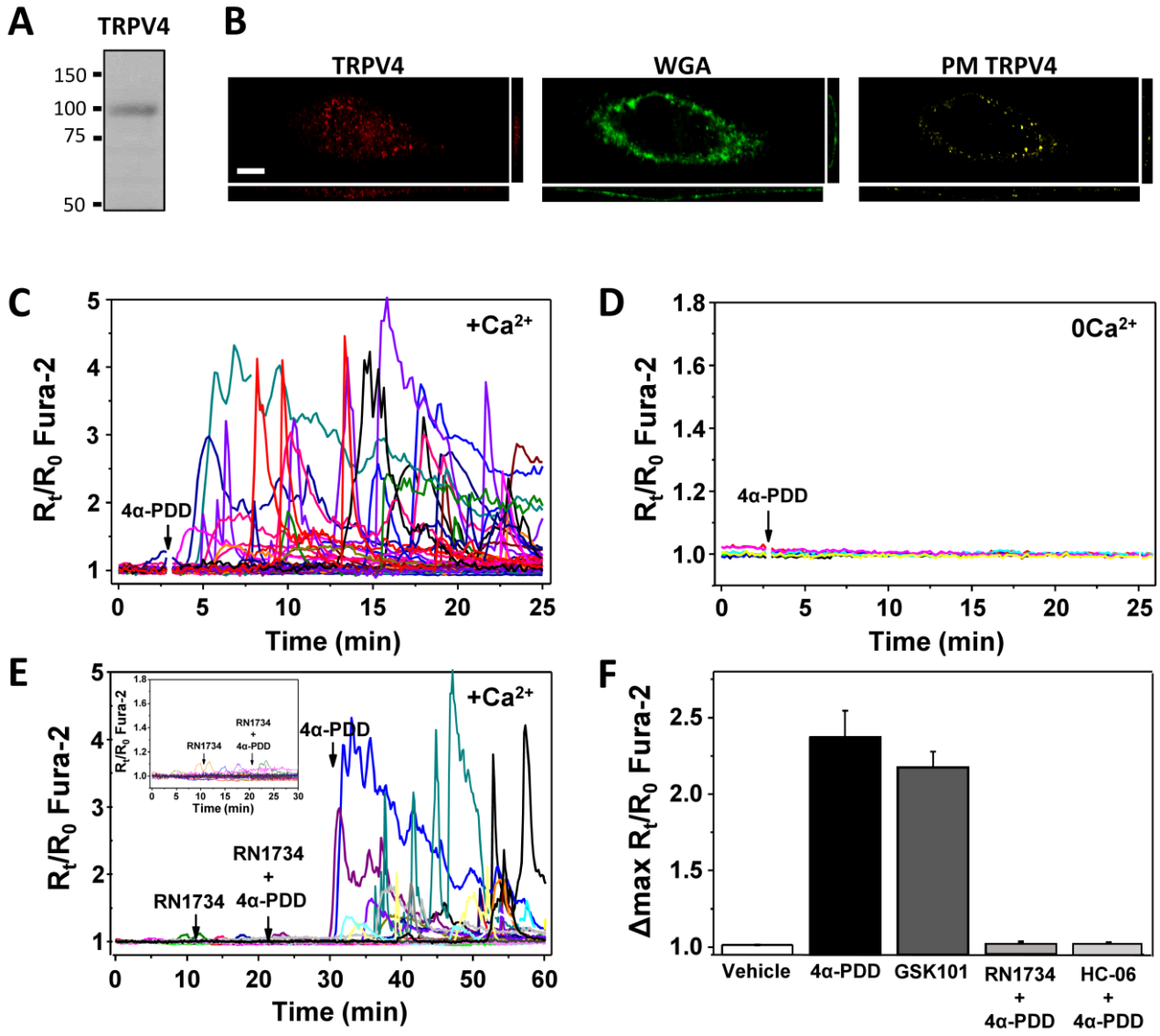

Figure 1

This article is protected by copyright. All rights reserved

Accepted Article

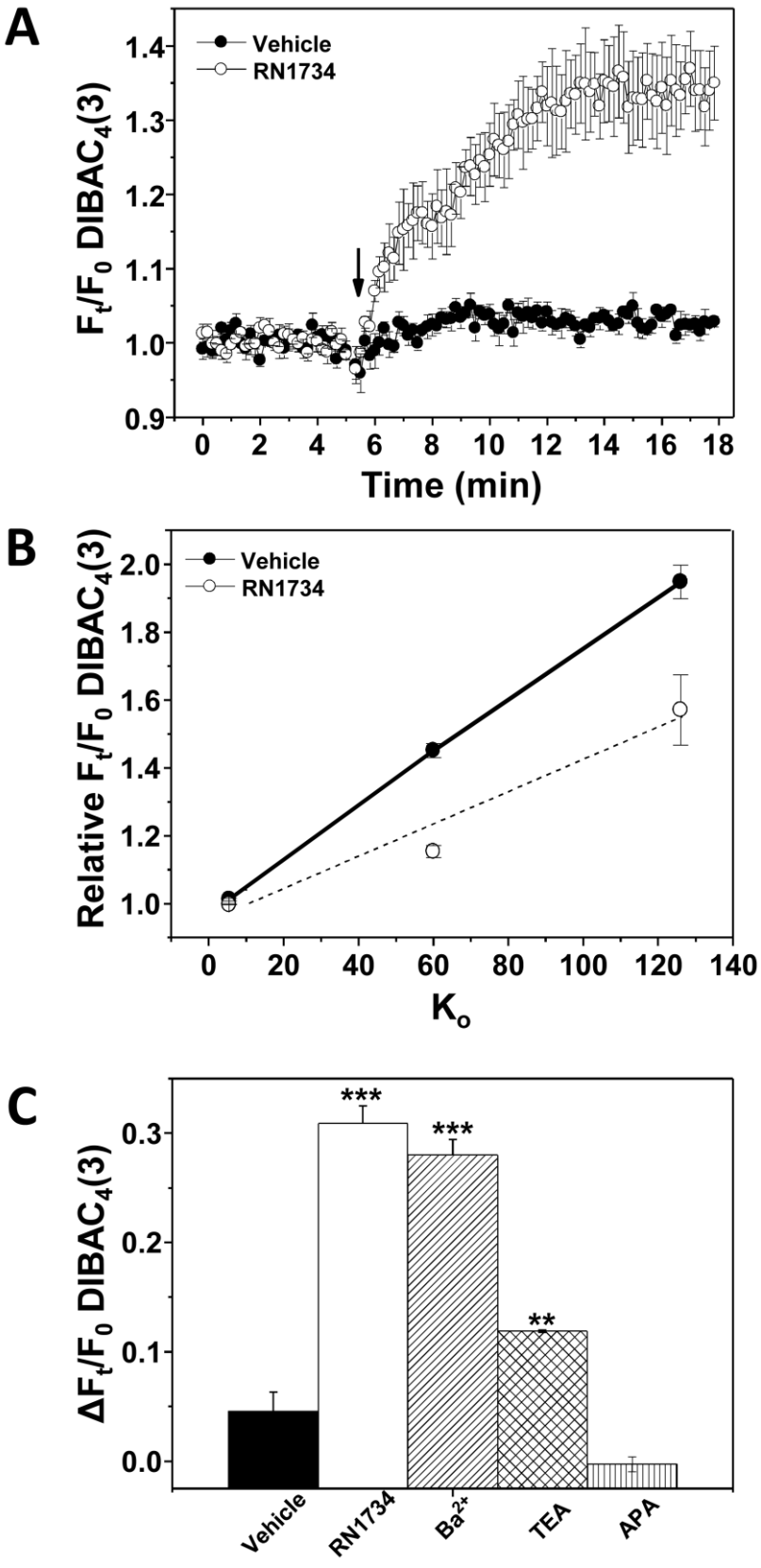

Figure 2

This article is protected by copyright. All rights reserved

Accepted Article

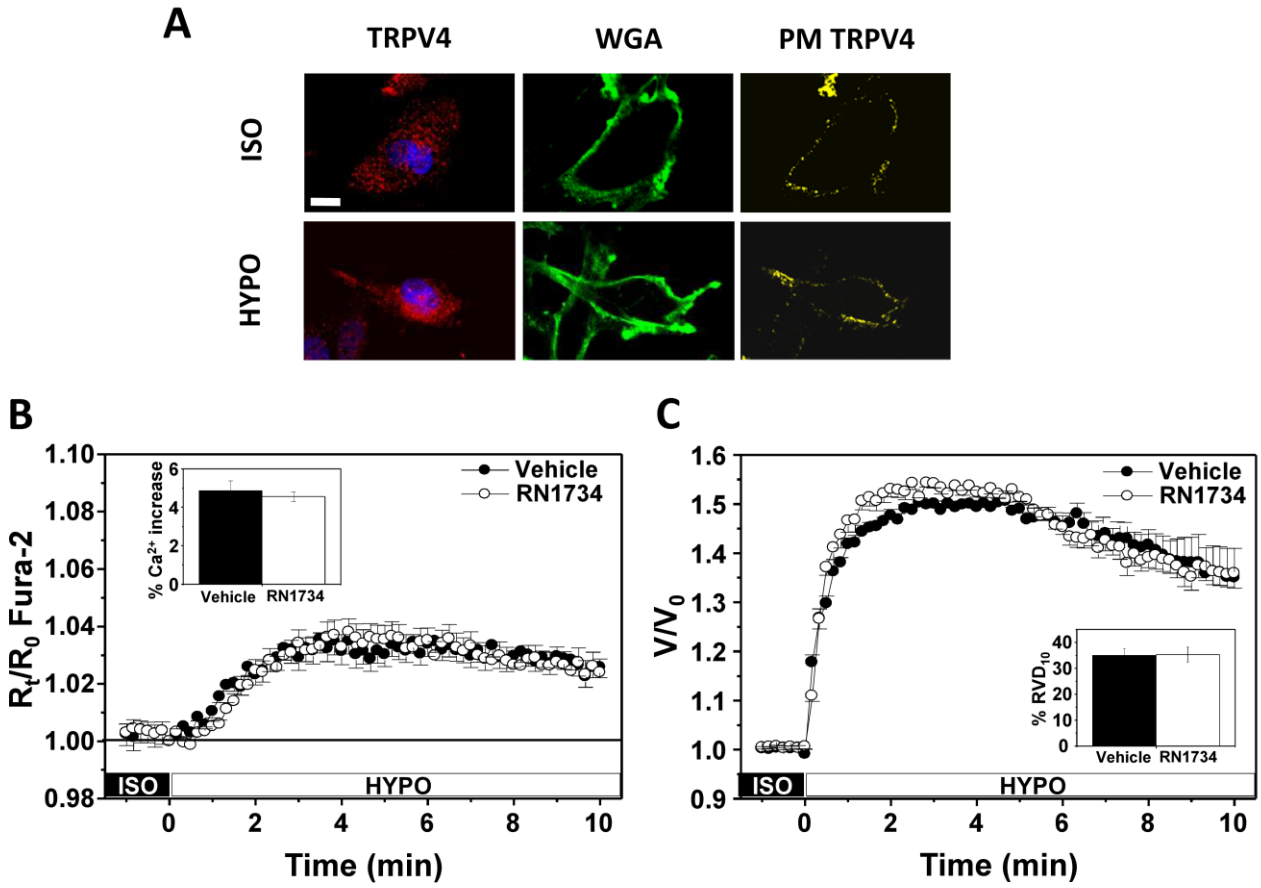

Figure 3

This article is protected by copyright. All rights reserved

Accepted Article

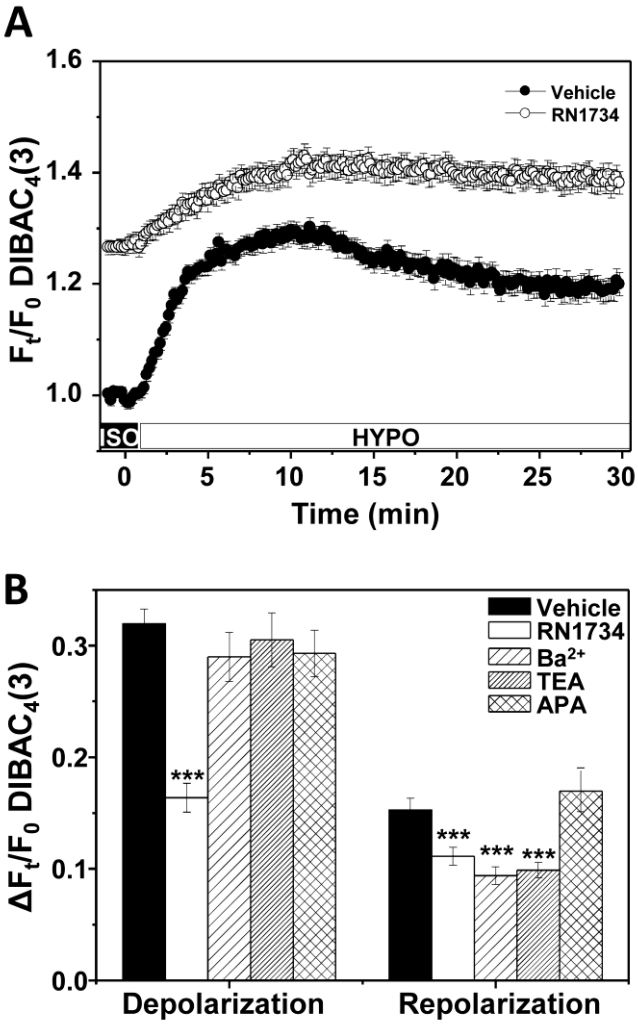

Figure 4

This article is protected by copyright. All rights reserved

Accepted Article

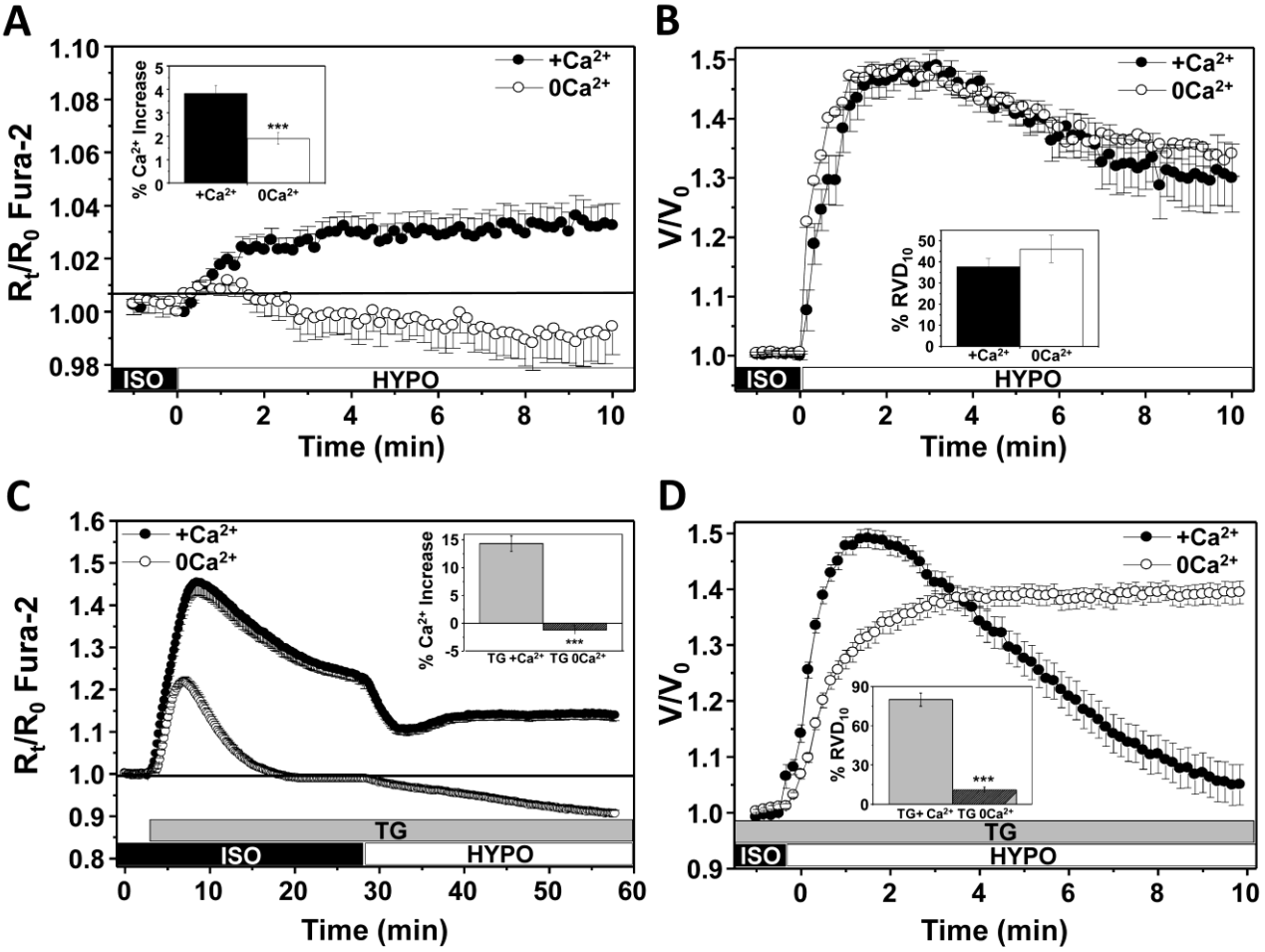

Figure 5

This article is protected by copyright. All rights reserved

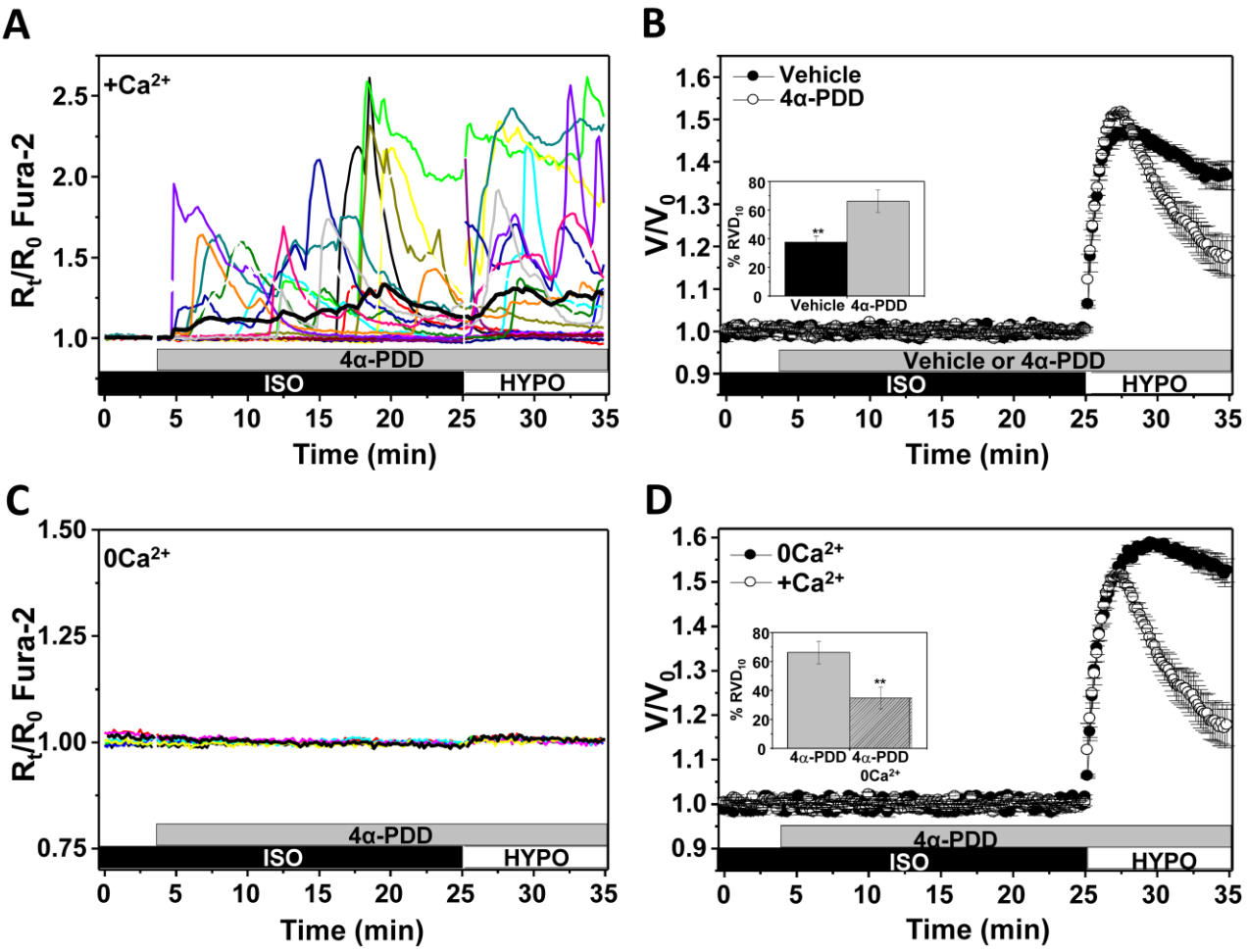

Figure 6

Accepted Article

This article is protected by copyright. All rights reserved

Accepted Article

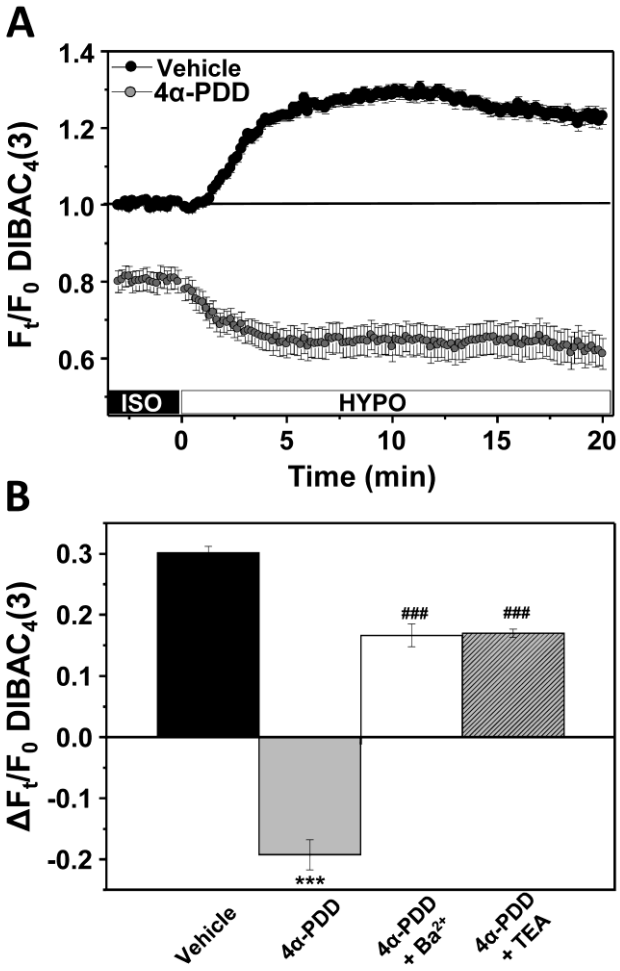

Figure 7

This article is protected by copyright. All rights reserved